



# Residence Time Distribution-Based Smith Predictor: an Advanced Feedback Control for Dead Time–Dominated Continuous Powder Blending Process

Martin Gyürkés<sup>1</sup> · Kornélia Tacsi<sup>1</sup> · Hajnalka Pataki<sup>1</sup> · Attila Farkas<sup>1</sup>

Accepted: 31 March 2023  
© The Author(s) 2023

## Abstract

**Purpose** In continuous manufacturing (CM), the material traceability and process dynamics can be investigated by residence time distribution (RTD). Many of the unit operations used in the pharma industry were characterized by dead time–dominated RTD. Even though feasible and proper feedback control is one of the many advantages of CM, its application is challenging in these cases. This study aims to develop a feedback control, implementing the RTD in a Smith predictor control structure in a continuous powder blender line.

**Methods** Continuous powder blending was investigated with near-infrared spectroscopy (NIR), and the blending was controlled through a volumetric feeder. A MATLAB GUI was developed to calculate and control the concentration of the API based on the chemometric evaluation of the spectra. The programmed GUI changed the feeding rate based on the proportional integral derivative (PID) and the Smith predictor, which implemented the RTD of the system. The control structures were compared even on a system with amplified dead time.

**Results** In this work, the control structure of the Smith control was devised by utilizing the RTD of the system. The Smith control was compared to a classic PI control structure on the normal system and on an increased dead time system. The Smith predictor was able to reduce the response time for various disturbances by up to 50%, and the dead time had a lower effect on the control.

**Conclusions** Implementing the RTD models in the control structure improved the process design and further expanded the wide range of applications of the RTD models. Both control structures were able to reduce the effect of disturbances on the system; however, the Smith predictor presented more reliable and faster control, with a wider space for control tuning.

**Keywords** Residence time distribution · Advanced feedback control · Smith predictor · Continuous manufacturing · Twin-screw powder blending · Process modeling

## Abbreviations

RTD	Residence time distribution	ICH	International Conference on Harmonization
PID	Proportional integral derivative control	QbD	Quality-by-design
PI	Proportional integral control	PDF	Probability distribution function
DT	Dead time	CDF	Cumulative distribution function
CM	Continuous manufacturing	TIS	Tank-in-series model
FDA	US Food and Drug Administration	CQA	Critical quality attribute
PAT	Process analytical technology	CPP	Critical process parameter
NIR	Near-infrared spectroscopy	API	Active pharmaceutical ingredient
		MPC	Model predictive control
		ASA	Acetylsalicylic acid
		MCC	Microcrystalline cellulose
		CU	Content uniformity
		LIW	Loss-in-weight
		GIW	Gain-in-weight
		PLS	Partial least squares
		GUI	Graphical user interface

✉ Attila Farkas  
farkas.attila@vbk.bme.hu

<sup>1</sup> Department of Organic Chemistry and Technology, Faculty of Chemical Technology and Biotechnology, Budapest University of Technology and Economics, Műegyetem Rkp. 3, 1111 Budapest, Hungary

AUC	Area under curve
MRT	Mean residence time
SSE	Sum of square errors

## Introduction

In recent years, continuous manufacturing (CM) gained increased interest in the pharmaceutical industry. Due to several reasons, including the strict regulatory environment created by authorities, the industry stuck with batch systems longer than other industrial fields. The US Food and Drug Administration (FDA) introduced a new risk-based approach with process analytical technology (PAT) [1], which helped the pharmaceutical industry to recognize the advantages of CM. The guideline proposed PAT tools to provide an initiative for development without intensive product testing [2], using fast analytical methods with at-line, on-line, and in-line methods, which are named based on the requirement of sampling (at-line, on-line) and sample pretreatment (at-line). In-line methods are the most advanced, as they are non-destructive and can measure the production line directly without sampling. The studied non-destructive solid-state methods, in particular, vibrational spectroscopic methods, such as near-infrared spectroscopy (NIR) and Raman spectroscopy, provided excellent results as fast, in-line applicable and reliable methods [3–6].

The International Conference on Harmonization (ICH) responded as they described the quality-by-design (QbD) principles in the ICH Q8 guideline [7]. While the PAT framework is applicable to batch technologies, it supports innovation, and the improvement in process monitoring capability guided the innovation of CM [8]. After extensive research showcased the benefits of CM [9–11] and its execution [12, 13], several drugs have been successfully approved using CM and presented benefits even during the regulatory submissions in the USA [14]. While these comparisons may have a bias in favor of CM, the industry is interested in the implementation, as according to Fisher et al. [14], the pharmaceutical CM market doubled between 2016 and 2020. These results led both the ICH and the FDA to present drafts of CM frameworks [15, 16].

The role of process understanding and modeling play a more pivotal role in CM than in batch processes, as modeling can explain the required definitions of the process in the CM realm and face the challenges of the paradigm shift [15, 16]. Both frameworks refer to the residence time distribution (RTD) as the most common approach to access process dynamics. The literature of RTD in solid operations has substantially grown in recent years [17, 18]. Examples of RTD measurements for the most common continuous unit operations have been presented. Powder blending is one of the most researched unit operations for RTD studies [19–26],

besides wet granulation [27–31] and tableting feed frames [32–34]. Most recently, examples describing the investigation of RTD of integrated processes have been published [35–39]. In many cases, the disturbances can only be measured after a significant dead time, which can be related to the plug flow region of the processes, where the materials travel without back mixing [19, 31, 32, 36, 37, 39].

In most cases, the RTD is measured with impulse or step disturbances through tracer experiments [17, 18, 24]. These are straightforward methods to determine the probability distribution function (PDF) or the cumulative distribution function (CDF), as the response functions of impulse disturbance correlate to the PDF, while the response function of step disturbance corresponds to the CDF [24]. Process models, such as tank-in-series (TIS) and axial dispersion models, often with the implementation of dead time to describe the plug flow region, have been directly imported from liquid operations, as they work properly for solid operations [17, 18, 26].

Continuous manufacturing also requires feasible process control application. Process control is named one of the four main concepts of the PAT framework [1]. However, the Q13 draft guideline does not mention active process control, such as feedback or feedforward control. Nevertheless, the scientific approaches chapter includes an in-depth description of the applicable control strategy [15]. The guideline describes the requirement of process monitoring, and the common approaches of control are listed as the establishment of target setpoints and control limits, design space, and specifications for attributes being measured [15]. The control strategy is described in detail even in the CM guidance of the FDA [16]. The guidance covers material diversion, real-time release testing, trend analysis, and specifications and describes active process control, including automated feedforward/feedback controls as well [16].

Most publications address the question of control strategy with material diversion and by setting control limits with advanced methods that include calculating with the RTD and using funnel plots [23, 35, 39–45]. Active process control based on PAT tools is used less frequently on an entire system, meaning that product's critical quality attributes (CQAs) are rarely coupled with active control structures [46]. Most equipment is equipped with PLC controllers. Feeders implement different control structures, from which gravimetric feeders, the best available tools for achieving reliable feeding, keep the set feeder rate based on PID controls of the change of mass [47, 48], and even ratio controllers are used in feeder systems when the set point of one feeder is dynamically changed based on the output of other feeders [49, 50]. Drying air temperature, air flow, equipment temperature, and basically every critical process parameter (CPP) is controlled. Still, in most cases, these parameters are adjusted to a defined setpoint, and measured CQAs are only used to determine if the analyzed product is eligible or

should be discarded. In an active process control structure, the PAT measurements should be used to control the CPPs to achieve controlled CQAs. An example of PI control is presented by Nagy et al. [51], controlling the feeder of a powder blending setup based on the active pharmaceutical ingredient (API) concentration. Reimers et al. [52] have used a PI control system in a fluid bed granulation process. Several publications work with model predictive control (MPC) [53] applications in a hybrid [54–56] and nonlinear modeling [57]. Rehr et al. [58] connected the RTD models with an MPC control structure. However, the control used linearization and was tested on a space-state model instead of a real-world system.

All of the examples used PI control systems without the derivative component or MPC control. This is because many pharmaceutical CM processes are dead time–dominated, meaning that the time until the disturbances first appear in the product is relatively high compared to the width of the RTD and the measurement frequency. Smith predictor [59–62] was introduced to compensate for the destabilizing effect of dead time, using a model-based control structure. This powerful control structure is used in many fields; however, according to the authors' knowledge, it lacks pharmaceutical applications.

In this study, an application of Smith predictor is presented in pharmaceutical manufacturing. The work is intended to couple the Smith predictor with the RTD of the powder blending as the model of the system, expanding the applications of the RTD models as an important tool for process design. In the scope of this study, the RTD-based Smith predictor is compared to the traditional PID control. This approach is not limited to powder blending applications. The presented structure provides an applicable and manageable control structure to dead time–dominant process dynamics, with the mechanistic RTD model and the PID-based Smith predictor.

## Materials and Methods

### Materials

A two-component, direct compression compatible model system was selected containing an API and a tableting excipient. The API was crystalline acetylsalicylic acid (ASA) (particle size:  $d_{10} = 133.16 \mu\text{m}$ ;  $d_{50} = 532.86 \mu\text{m}$ ;  $d_{90} = 1223.77 \mu\text{m}$ ) marketed as Rhodine 3040 (Novacyl, France). The tableting excipient was microcrystalline cellulose (MCC) marketed as Vivapur 200 (particle size:  $d_{10} = 113.88 \mu\text{m}$ ;  $d_{50} = 247.93 \mu\text{m}$ ;  $d_{90} = 449.58 \mu\text{m}$ ), bought from JRS Pharma GmbH (Germany). The two components were mixed in a ratio of 20% ASA to 80% MCC, but the ratio was changed in some measurements to provide disturbance for the system.

### Continuous Powder Blending Setup

The investigated powder blending is the same process that we used in the paper of Gyürkés et al. [23] (Fig. 1A). In continuous lines, the ingredients are simultaneously and continuously fed into a blender to ensure proper blend uniformity for the subsequent operations. The MCC was fed with a twin-screw gravimetric feeder (Brabender loss-in-weight feeder, DDW-MD0-MT-1.5 HYD with Congrav OP 1 T operator interface). The screws have high capacity and oval geometry (9.0 mm × 11.5 mm).

The ASA was fed with a single-screw feeder (FPS Pharma, Fiorenzuola d'Arda, Italy), which has a round geometry and a lower feeding capacity. It is ideal for low mass flow rates. The feeder has no integrated scale or control system, but the rotation speed can be controlled via a serial connection.

The ASA and MCC were continuously blended in a TS16 QuickExtruder (Quick 2000 Ltd., Hungary) twin-screw multipurpose equipment using a 25 L/D ratio screw with 16 mm diameter. The equipment proved feasible for powder blending [19, 23, 51]. The screw contained conveying and kneading elements (Fig. 1B), but any changes in particle size and flow dynamics were not experienced. The excipients were fed with different feeders through the same feeding chute.

After the twin-screw blender, the product was collected on a conveyor belt, which was operated at 18 cm/min speed. The NIR probe was mounted on the conveyor belt. Generally, the probe was placed as close to the extruder die to achieve real-time results. However, in some measurements, the probe was placed 15 cm from the die modeling process with a longer dead time. The configuration, except the NIR probe in the aforementioned measurements, remained unchanged between the RTD and control measurements.

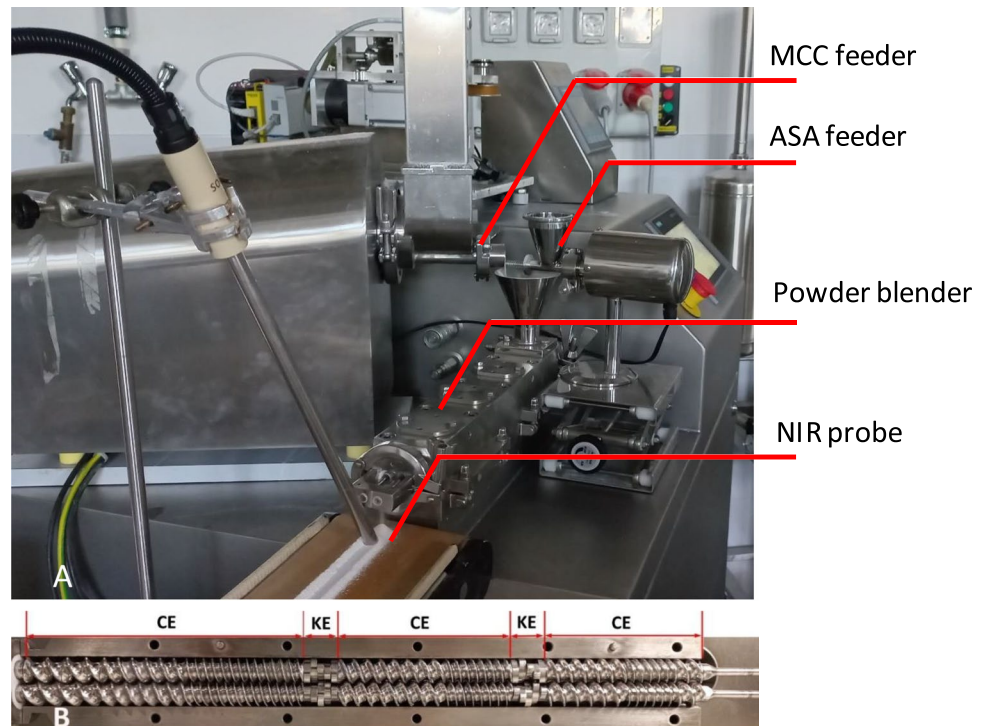
The prepared blends are simple formulations. More components may require further feeders or multiple coupled powder blending steps for more complicated formulations, which may also make the NIR models complicated.

### Feeder Profile

MCC was fed into the blender with the gravimetric loss-in-weight (LIW) feeder, which was controlled with the internal algorithm of the feeder. The feeding rate was measured and shown on a control panel. The feeder has an inbuilt calibration based on a lower and higher feeding rate.

However, the ASA was fed with a volumetric feeder, which has no inbuilt weight measurement but can be controlled externally. We have measured the feeder profile to use as a base for the control. The profile was measured offline, with a gain-in-weight (GIW) setup, and in-line with the continuous powder blending setup, measured with the NIR probe.

**Fig. 1** **A** Powder blending setup and **B** screw configuration



The GIW setup consisted of the feeder and an analytical scale (Sartorius L420P). The analytical scale was placed under the feeder, catching the fed ASA. The feeder was controlled externally, setting the speed of the feeder uniformly, reading the weight after the feeder was set at the controlled speed, and reading the GIW every minute for 3 min. The intermediate settings were calculated with the linear fit between two measurements.

### NIR Spectrometry and Data Analysis

NIR spectrometry was utilized for the characterization of the process and as the input sensor in the feedback control loop. Bruker MPA FT-NIR spectrometer (Bruker Optik GmbH, Germany) was equipped with a Solvias fiber optic probe (Solvias AG, Switzerland) in reflection mode. NIR spectra were collected with  $8\text{ cm}^{-1}$  resolution at the range of  $4000\text{--}12,500\text{ cm}^{-1}$ . In the case of calibration, 16 scans were accumulated for each measurement, while in the case of real-time measurements, the spectra were collected without accumulation; therefore, the spectra collection was less than 4 s. The concentration was calculated from the spectra with the PLS calibration used by Gyürkés et al. [23].

The measured concentration curves were smoothed for visualization and quantification purposes but were not used for control. Smoothing was achieved with Savitzky-Golay smoothing based on a 15-data point window and second polynomial order. The controller used the raw data, but the performance of the controller is presented based on the

smoothed curve. Smoothing was necessary to reduce the imperfections caused by the fast acquisition time, which derives not only from the inaccuracy of the NIR evaluation but also from the small spot size and, therefore, not representative sample size caused by the NIR probe.

Spectra were collected by OPUS 7.5 software (Bruker). The spectra were evaluated by MATLAB R2020b (9.9, Mathworks, USA) and PLS Toolbox 8.7.1. (Eigenvector Research, USA). The concentration monitoring and control were carried out by in-house developed MATLAB graphical user interfaces (GUI). The GUI runs in real-time, reading the spectra from files, then calculating the concentration with predefined partial least squares (PLS) models. The GUI calculates the control action based on PID control loop and in the case of Smith-predictor based on predefined RTD models and, finally, controls the feeder through a serial connection.

### Determination of Residence Time Distribution

The RTD of the continuous powder blender setup was measured with impulse disturbances. MCC was continuously fed to the hopper with gravimetric feeding. Pure ASA was manually added to the system directly into the hopper. To minimize the error generated by the added ASA, the impulse size was set to 0.2 g.

The blend product was measured spectroscopically in real time, and the response function was measured with the GUI by starting a timer at the time of the disturbance and collecting the calculated concentrations.

The response function corresponds to the probability distribution function (PDF) of the RTD after baseline correction and normalization, which was done by dividing the response with the area under curve (AUC) (Eq. 1). The main parameters of the RTD were calculated from the moments (Eqs. 2-4) of the response function calculated with numerical integrations.

$$E(t) = \frac{c(t) - c(0)}{\int_0^\infty (c(t) - c(0))dt'} \tag{1}$$

$$MRT = \int_0^\infty t \cdot E(t) \cdot dt, \tag{2}$$

$$Var = \int_0^\infty (t - MRT)^2 \cdot E(t) \cdot dt, \tag{3}$$

$$\sigma = \sqrt{Var}, \tag{4}$$

where E(t) is the probability distribution function (PDF) of the process in t as time, c(t) is the measured concentration in t, MRT is the mean residence time of the PDF, Var is the variance of the PDF, and σ is the standard deviation of the PDF.

### Residence Time Distribution Modeling

The modeling was done with the least squares method after preprocessing of the measured responses.

The preprocessing contained a baseline correction to adjust the bias of the PLS model at zero concentration. The baseline correction is also needed if the concentration before and after the impulse disturbance is not zero, i.e., when the disturbance is done with a pre-blend or during normal operation, with all ingredients fed simultaneously. After the baseline correction, the responses were normalized by numerical integration. The preprocessing was done according to Eq. (1) and directly resulted in the measured PDF.

Tank-in-series (TIS) models were used for RTD modeling. The model is described in Eqs. (5 and 6). Plug flow attribute was described with a dead time (t<sub>D</sub>). The TIS-like behavior was described with two additional parameters using equal size tanks, the number of the tank (N), and the MRT of the total system (τ<sub>TIS</sub>).

$$E_{TIS}(t) = \frac{N \cdot e^{-\frac{t-t_D}{\tau_{Tank}}} \cdot \left(\frac{t-t_D}{\tau_{Tank}}\right)^{N-1}}{\tau_{TIS} \cdot (N-1)!}, \tag{5}$$

$$\tau_{Tank} = \frac{\tau_{TIS} - t_D}{N}, \tag{6}$$

where E<sub>TIS</sub> is the PDF based on the TIS model and τ<sub>Tank</sub> is the MRT of one individual Tank.

The least squares method was accomplished by finding the minimum of the sum of squared error (SSE), calculated based on Eq. (7), by changing the value of the three parameters of the TIS model.

$$SSE = \sum_{i=1}^n \left[ E_{TIS}(t)|_{t_i} - E(i) \right]^2, \tag{7}$$

where i refers to the ith measurement at t<sub>i</sub> time.

### Feedback Control

Two control structures were compared, the simple PI(D) control and the advanced control structure of the Smith predictor. Figure 2 presents the PI(D) control structure, in which the controller calculated the actual feeder speed based on Eqs. (8 and 9).

$$Er(t) = SP(t) - c(t), \tag{8}$$

$$F(t) = B(SP(t)) + K_P \cdot Er(t) + K_I \cdot \int_0^t Er(t)dt + K_D \cdot \frac{\Delta Er(t)}{\Delta t}, \tag{9}$$

where Er(t) is the error in t time, SP(t) is the setpoint at t time, and c(t) is the concentration at t time calculated from the NIR spectrum. The controller calculates F(t) as the feeder speed at t, from B(SP(t)) as the base value, calculated from the actual setpoint based on the feeder profile, and K<sub>P</sub>, K<sub>I</sub>, and K<sub>D</sub> are the gains of the P, I, and D components of the PID controller.

The control structure of the Smith predictor has depicted in Fig. 3. The control is the same PID control as in the previous case, but a complex model computed the error values as follows. The model predicted the concentration at the time of the measurement based on the collected feeder speed. This predicted concentration corresponds to earlier feeder speeds due to the effect of RTD. However, the effect of

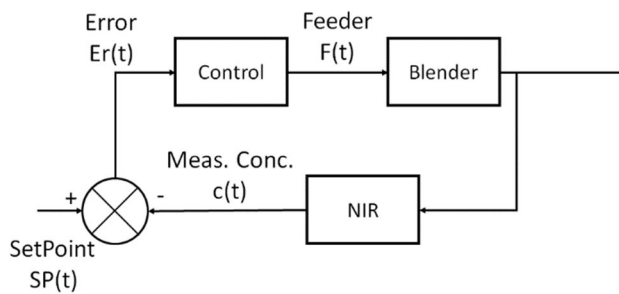
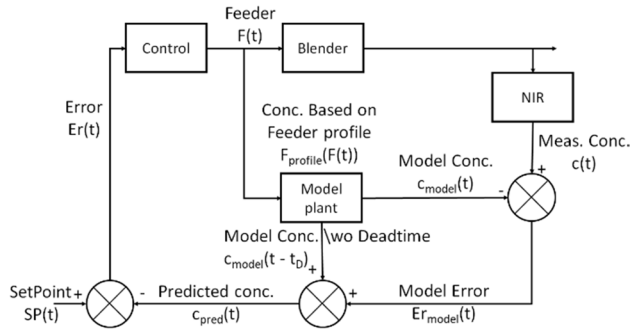


Fig. 2 PID control structure



**Fig. 3** Smith predictor control structure

recent feeder speeds is also predicted with the same model, but with the elimination of the dead time. The input of the controller is calculated based on the model error (measured concentration—model predicted concentration), added to the predicted effect of the actual feeder speeds, and subtracted from the setpoint. The calculation is described in Eqs. (10–13).

$$c_{model}(t) = F_{profile}(F(t)) \times E(t'), \quad (10)$$

$$Er_{model}(t) = c(t) - c_{model}(t), \quad (11)$$

$$c_{pred}(t) = c_{model}(t - t_D) + Er_{model}(t), \quad (12)$$

$$Er(t) = SP(t) - c_{pred}(t), \quad (13)$$

where  $c_{model}(t)$  is the calculated concentration based on the feeder input ( $F(t)$ ), corrected with the feeder profile ( $F_{profile}(x)$ ) and convolved with the PDF of the measured RTD ( $E(t')$ ).  $Er_{model}(t)$  is the model error.  $c_{pred}(t)$  is the Smith-predicted concentration, which is the model concentration without dead time, corrected with the model error. Finally, the PID control is the same as in Eq. (9), using the error calculated with Eq. (13).

## Control Tuning

Tuning a control loop is an intensive and important part of implementing feedback control. However, the tuned parameters have to be selected according to the system, the limits of the system, and the anticipated deviations. Some systems may be more sensitive for higher but shorter impulses and tolerate long-term, low amplitude deviation better, whereas the opposite may be true for other systems. Therefore, in some cases, slower but robust control tuning is more feasible than faster, aggressive setups [63]. The Smith predictor has been criticized lately because the control structure is more complicated due to the model, while the improved performance can

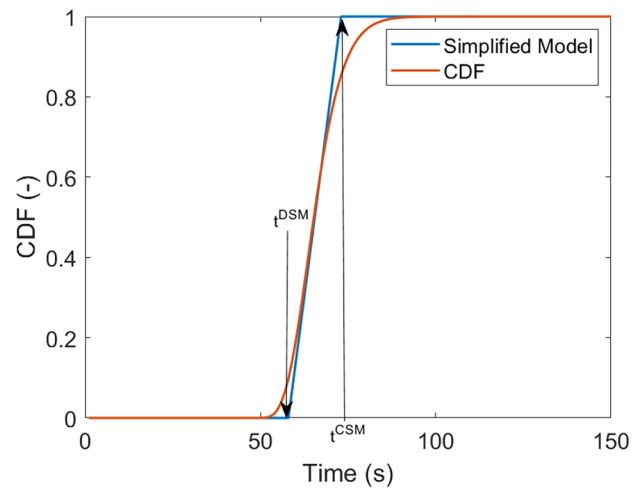


**Fig. 4** Fit and parameters of the simplified model, used for control tuning

be marginal [63, 64]. However, it is an applicable alternative if PID fails and provides a clear and understandable control when it is combined with the process dynamics.

Intensive control tuning can be achieved by multiple methods, using labor-intensive trial-and-error method, simple rule based methods such as Ziegler-Nichols tuning. The most accurate methods are optimization-based methods, using mathematical optimization, but these are computationally intensive algorithms and require reliable process models. Nevertheless, the tuned parameters require validation and further adjustments.

In the scope of this publication, we were interested in the feasibility of the RTD model-based Smith predictor and the relation between the two control setups. Therefore, a simple tuning method was used based on the simplified open-loop transfer function. The tuning was feasible as the plant does not contain integrating parts.

CDF of the RTD was used as the open-loop transfer function of the system. The function was simplified to a first-order system, by fitting a linear model on the CDF, which was described by the simplified model dead time ( $t_{DSM}$ ) and the simplified model time constant ( $t_{CSM}$ ). The fitting is presented in Fig. 4. The control parameters were calculated from two time constants based on Table 1 [65]. For the Smith predictor, the same tuning was used, except that the dead time of the controller was subtracted from the time constants. This method makes the dead time of the Smith predictor an additional parameter of the control structure, which determines the control gains.

**Table 1** Recommended control gains based on the simple tuning

	$K_P$	$K_I$	$K_D$
<b>PI</b>	$\leq \frac{T_{CSM}}{T_{DSM}}$	$\leq \frac{K_P}{3.3 \cdot T_{DSM}}$	0

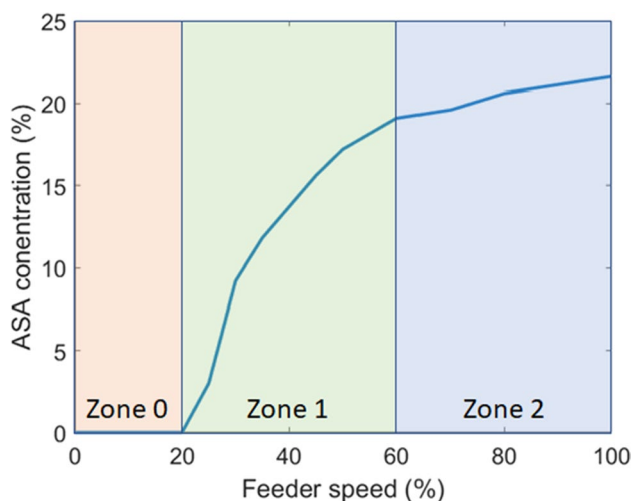


**Fig. 5** Feeding profile of the ASA feeder. Zone 1 is feasible for control; Zone 2 is more stable

## Results and Discussion

### Feeder Profile

The feeder profile of the ASA feeder was measured with the GIW feeder and scale setup. The current to the feeder was changed percentwise with predefined set of feeder speed values. The feeder screw only started moving from 20%; therefore, the calibration was done on 7 settings (20%, 30%, 40%, 50%, 60%, 70%, and 100%).

First, the feeder was filled, and then a low percentage (30%) was selected to fill the feeder screws. After filling the screws, when the feeding rate stabilized, calibration started. The feeder was set to the proper feeder current, the ASA was fed for 30 s, to achieve a controlled state, and then the mass was recorded by a scale every minute for 3 min. The feeder rates at different currents are presented in Fig. 5.

The feeder has a nonlinear profile, where the feeding only starts at 20% or higher current and between 20 and 60% changes rapidly. However, after 60% of the maximum current, the change in feeding rate suddenly slows down. Between 70 and 100%, the screw cannot transport more ASA; thus, the feeding rate barely changes. For the control measurements, we had to select an applicable feeding rate.

The feeder operated in two zones above the minimum current required (Fig. 5). The first zone is better for feedback control, because, in this zone, the controller has a higher effect on the system, as smaller changes correspond to higher intervention. This way, the controller is capable of responding to disturbances in each direction.

The second zone is a stable zone, where the feeding rate barely reacts to changes in the feeder current. When the feeder is not controlled or high amplitude disturbances are

not expected, then this zone would offer better stability for commercial manufacturing. This zone has a lower reliance on the stability of the current.

Even though the feeder was calibrated, the base calculation of the controller was not perfect in each experiment; however, this imperfection was used as the first disturbance to test the control structures.

### Residence Time Distribution

The RTD of the system was measured before every control experiment. The measurement was done with impulse disturbances, repeated three times. The impulse responses were collected, baseline corrected, and normalized with the AUC normalization. Finally, a TIS model was fitted with least squares method (Fig. 6a), which can be defined with the parameters presented in Table 2.

The RTD has been manipulated to simulate a manufacturing where the dead time is even higher compared to the time constant. For this, the probe was mounted 15 cm away from the powder blender's die on the conveyor belt. The transfer on the conveyor belt modeled a plug flow region in the system (Fig. 6b).

The RTD measurement was reliable and did not change significantly in the system. However, the movement of the probe increased the dead time drastically. The profile of the two PDFs was similar, not insisting system wide differences after correction with the Smith dead time (Fig. 7).

### PI Control Experiments

The controller was tested with two different methods with the plant. After setting up the system, the RTD of the powder blender was measured. Two system setups were assessed. One with the NIR probe immediately after the blender is called the "normal" system. In contrast, another setup was investigated, where the probe was further away on the conveyor belt, which is called the "increased DT" system. The two methods for the controller testing differed in the disturbance. In the first case, the feeding speed of the excipient (MCC) was changed from 0.3 to 0.4 kg/h, which caused a decrease in the concentration after the lag due to the RTD. In the other method, the setpoint of the ASA concentration was changed from 15 to 10% on the controller. This has an immediate effect on the controller.

The smoothed concentration curve was analyzed for the qualification of the controls. The curves are presented with the 25% specification limits based on the USP standards. However, the performance was calculated based on the 10% action limits, and the change of the I part of the controller, a set time, and the ratio were determined when the concentration was out of the action limit. Set time is the

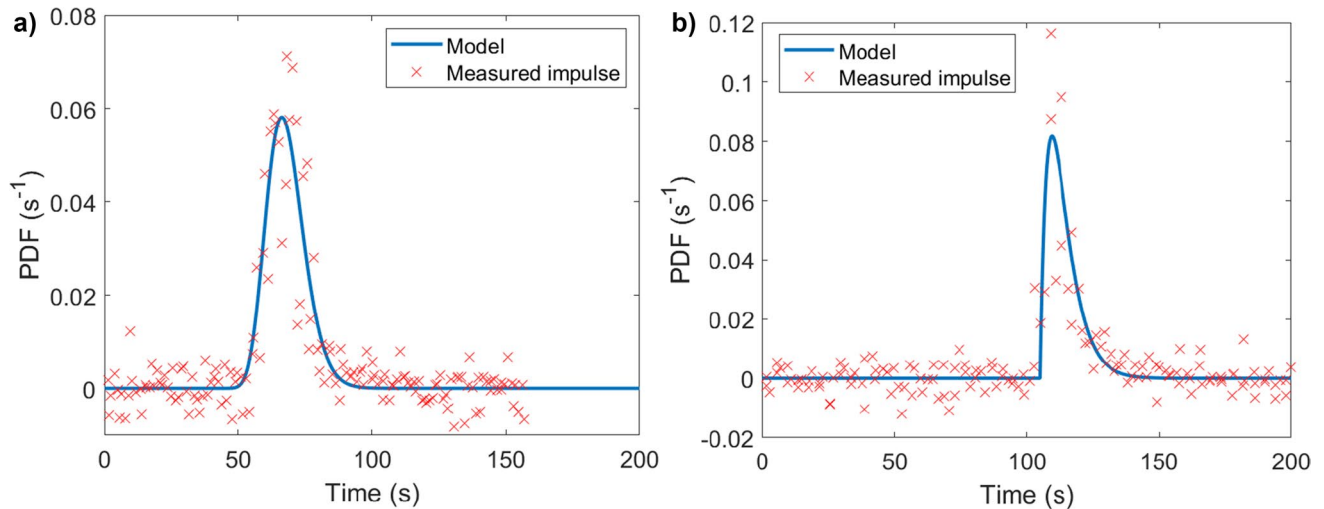


**Fig. 6** Probability distribution function of the normal **a** and the increased dead time **b** setup

**Table 2** Parameters of the measured RTD on the normal and the increased dead time system

System	MRT (s)	N (#)	DT (s)	$\sigma$ (s)	DT/MRT	$\sigma/DT$
Normal	68	17	39	7.03	0.574	0.180
Increased dead time	114	2	105	6.35	0.921	0.061

time needed to adjust the I part of the controller, while the ratio is the ratio of the time after a disturbance when the product was out of the action limits based on the 10% concentration limits.

The plant is dominated by a high dead time, as presented before. The startup phase was not controlled by the PI controller, because the integrated error from 0 concentration to the set concentration would offset the control for a long time. For the startup, the controller was used with 0 gains

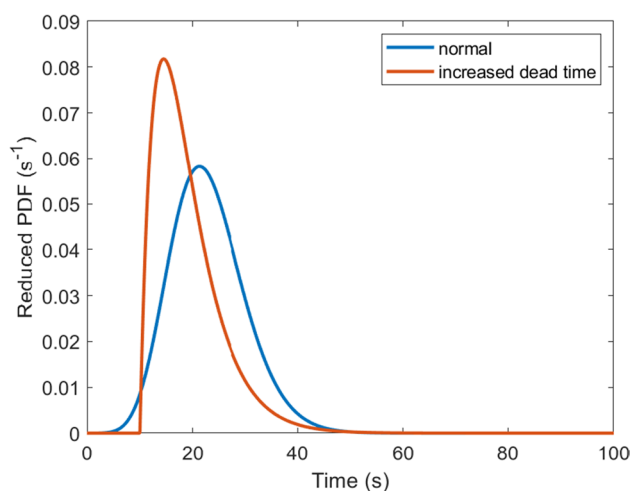


**Fig. 7** Probability distribution function of the two setups after correction with the dead time, which is used in the Smith predictor

for each component of the controller; therefore, the feeder was set to the base value calculated from the feeder profile.

After the base value was maintained at a constant concentration level, the gains were modified to the values calculated with the control tuning ( $K_p = 0.3$ ;  $K_I = 0.0015$ ). We used a controller reset to restore the integrated error. Another disturbance was introduced after the controller successfully set the concentration at the setpoint. A significant disturbance was made by changing the MCC feeding from 0.3 to 0.4 kg/h (red vertical line). Compared to real-life disturbances, this step did not intend to model real situations. It lowered the concentration drastically, but it was a proper disturbance to test the control (Fig. 8A).

The control was stable but very slow. The base value was good at the start, the controller did not have to adjust the feed rate with the I part of the control. The MCC feeding was changed 220 s after the measurement started. The integral control increased over time but was unable to adjust the feeding even after 1000 s, and the product was out of action limits 71.3% of the time (Table 1).

However, the control proved to be stable; therefore, we have tried to increase the PI gains. The same experiment was repeated with increased gains ( $K_p = 0.6$ ;  $K_I = 0.01$ ). This time, the initial concentration was higher due to the different load on the feeder chute. After 370 s, the controller achieved a concentration between the 10% limit; however, it took the controller 660 s to adjust the concentration to the setpoint (33.1% out of action limit).



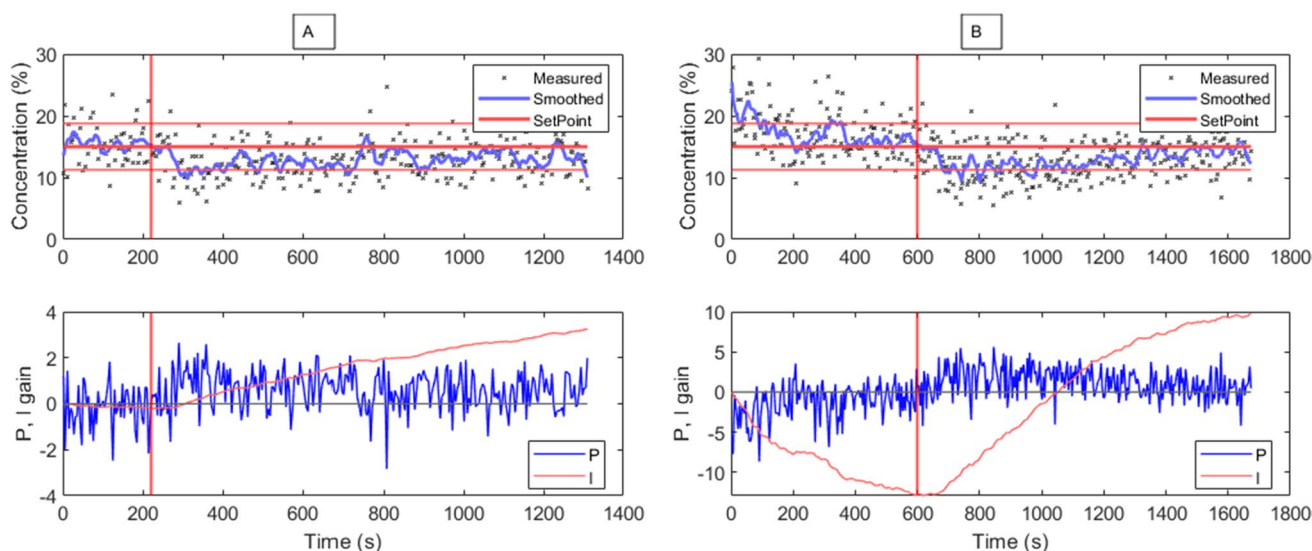


**Fig. 8** PI control of step change in MCC feeding (vertical red line) with **A** the recommended gains and **B** increased gains

After 600 s, the MCC feeding was changed from 0.3 to 0.4 kg/h (red line). The controller was able to adjust to the new feeding rate, but it took  $\sim 870$  s, and the product was out of action limits 69.2% of the time (Fig. 8B).

The same experiment was repeated with the increased dead time system; however, the control tuning calculated extremely low  $K_I$ , which was not tested. The system was tested on the increased gains ( $K_P = 0.6$ ;  $K_I = 0.01$ ). The concentration seemed to have settled with a small bias after 550 s ( $> 47.4\%$  out of action limit), and the MCC feeding was changed from 0.3 to 0.4 kg/h after 620 s. Despite the changed conditions, the integration part of the controller still decreased the feeding after the disturbance, as it did not stabilize properly before the disturbance. The controller slowly increased the ASA feeding after the disturbance, but the concentration did not reach the setpoint after 10 min ( $> 48.1\%$  out of action limit) (Fig. 9).

In another experiment, the concentration setpoint was changed from 15 to 10% and back as another form of disturbance (Fig. 10). The experiment was only measured on the normal setup with the increased gains ( $K_P = 0.6$ ;  $K_I = 0.01$ ). The controller took over 360 s to adjust the initial error, with a ratio of 34.6%. The first setpoint change was adjusted after 230 s, with a low ratio (24.6%). After the second setpoint change, the controller had an overshoot, which was adjusted slowly, achieving a stable concentration after 350 s (30.8% out of action limit).

### Smith Predictor Control Experiments

The Smith predictor was tested with the same methodology; therefore, during startup, the plant was controlled, with 0 PI gains. When the concentration was set at a stable, controlled

level, the controller gains were adjusted to the previously determined tuned parameters, and the integrated error was restored with the controller reset.

The controller was used to adjust the difference between the concentration at the calculated base level and the setpoint. The initial adjustment took 300 s (18.8% out of action limit). After the controller successfully set the system at the setpoint, the system was disturbed with the previously used MCC feeding rate change. The mass flow of the excipient increased from 0.3 kg/h to 0.4 kg/h at 430 s (vertical red line). The controller had a fast reaction time to the disturbances compared to the PI control and even to the RTD of the system. The concentration was adjusted just after 310 s;

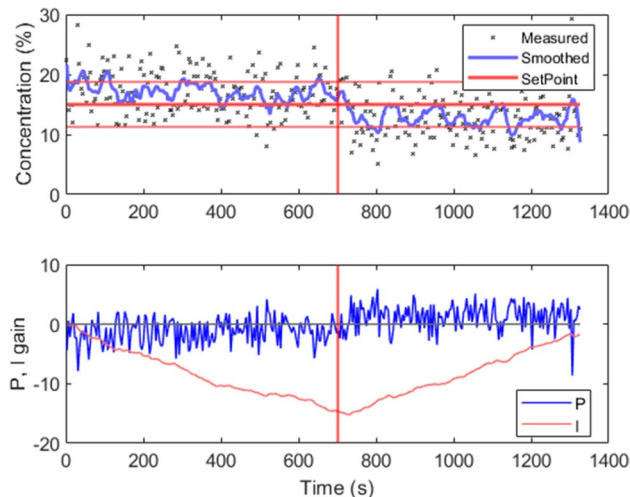


**Fig. 9** PI control for MCC step disturbance (vertical red line) on the increased dead time system

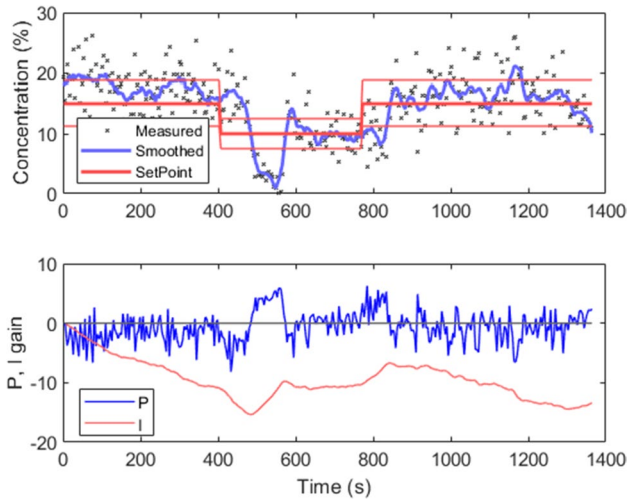


**Fig. 10** PI control of setpoint changes

however, the concentration kept decreasing, causing further deviations (44.4% out of action limit), but it was adjusted continuously (Fig. 11A).

The experiment was repeated with the increased dead time system. The controller reduced the initial concentration to the setpoint after 220 s; however, the controller showed some signs of instability (40.7% out of action limit). The MCC feeding rate was increased after 700 s (vertical red line), and the controller adjusted the concentration in 570 s (41.0% out of action limit) (Fig. 11B).

The standard setup was also tested with setpoint changes, just as the PI control. The initial error was adjusted after

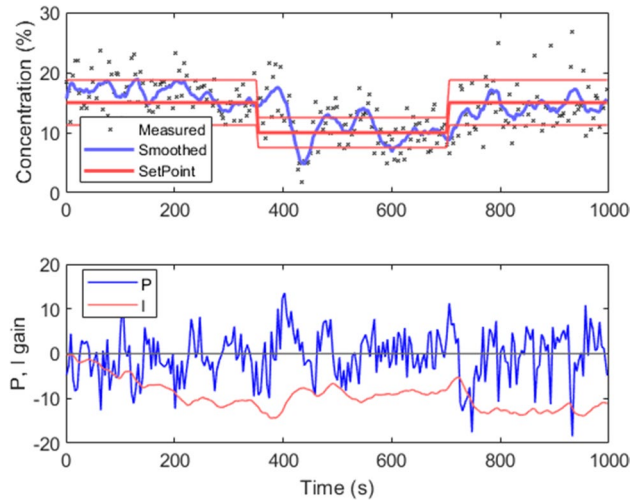


**Fig. 12** Response of the Smith predictor for setpoint changes

230 s (20.5% ratio). The first step change was adjusted after 280 s (23.3% ratio), while the second was adjusted just after 60 s (13.8% out of action limit) (Fig. 12).

The investigated control structures are compared in Table 3.

The two control strategies are compared in Fig. 13, with the disturbances adjusted to the 0 time point. In Fig. 13A, the step change in MCC feeding from 0.3 to 0.4 kg/h is compared, while in Fig. 13B, the step change of the setpoint from 15 to 10% is compared. In each case, the Smith had a faster reaction to the changes and achieved concentrations close to the setpoint almost immediately after the dead time of the system.

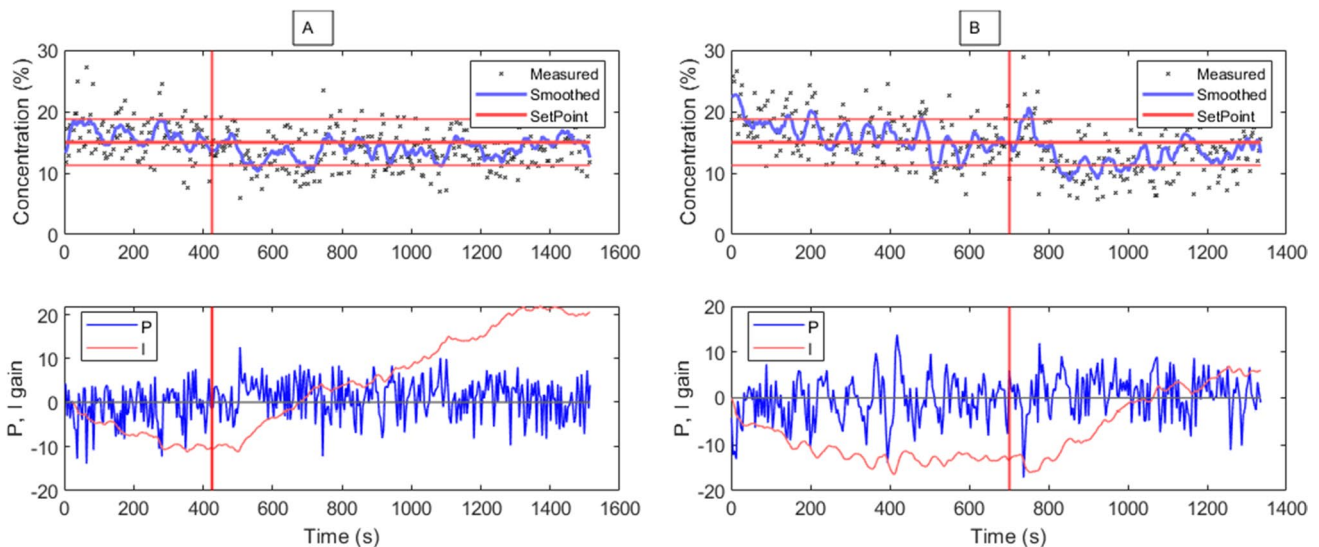


**Fig. 11** Application of the Smith predictor control structure to adjust the initial bias and the step disturbance of MCC feeding rate change (vertical red line) **A** on the normal system and **B** on the increased dead time system

**Table 3** Performance of the measured control structures on the normal and the increased dead time system, based on the set times (time needed to adjust the concentration to the setpoint) and the ratio of out of action limit on the first 1000 s period after disturbances

Control	$K_P$ ; $K_I$	System	Initial set time (s)	Set I gain	Ratio	Disturbance set time (s)	Set I gain	Ratio
PI	0.3; 0.0015	Normal	0	0	0.0%	> 1000	> 4	71.3%
PI	0.6; 0.01	Normal	660	- 12	33.1%	870	10	69.2%
PI	0.6; 0.01	Increased DT	550	- 15	47.4% <sup>a</sup> (64.3%)	> 700	> -1.5	48.1%* <sup>a</sup> (66.8%)
Smith	1.3; 0.03	Normal	300	- 10	18.8%	310	21	44.4%
Smith	1.2; 0.03	Increased DT	220	- 14	40.7%	570	6.4	41.0%
Step disturbances			Initial (s)	Ratio	First step (s)	Ratio	Second step (s)	Ratio
PI	0.6; 0.01	Normal	360	34.6%	230	24.6%	350	30.8%
Smith	1.3; 0.03	Normal	230	20.5%	280	23.3%	60	13.8%

<sup>a</sup>The control did not settle at the end of the measurement; therefore, the calculated ratio is lower than the real ratio and may be misleading

The dead time used for the Smith predictor acts as a new parameter for control tuning, which determined the level of the other parameters. We have tried to keep the proportional gain between 0.8 and 1.2 and the integral gain close to 0.03. This way, we could use an aggressive control compared to the PI control, while maintaining a stable control structure.

Due to the aggressive control, the disturbances were corrected quickly, but the control also induced some error in time. During some disturbances, the control was close to the stability limit, but the control proved to react faster than the PI control and has more opportunity to achieve stable control even with aggressive tuning.

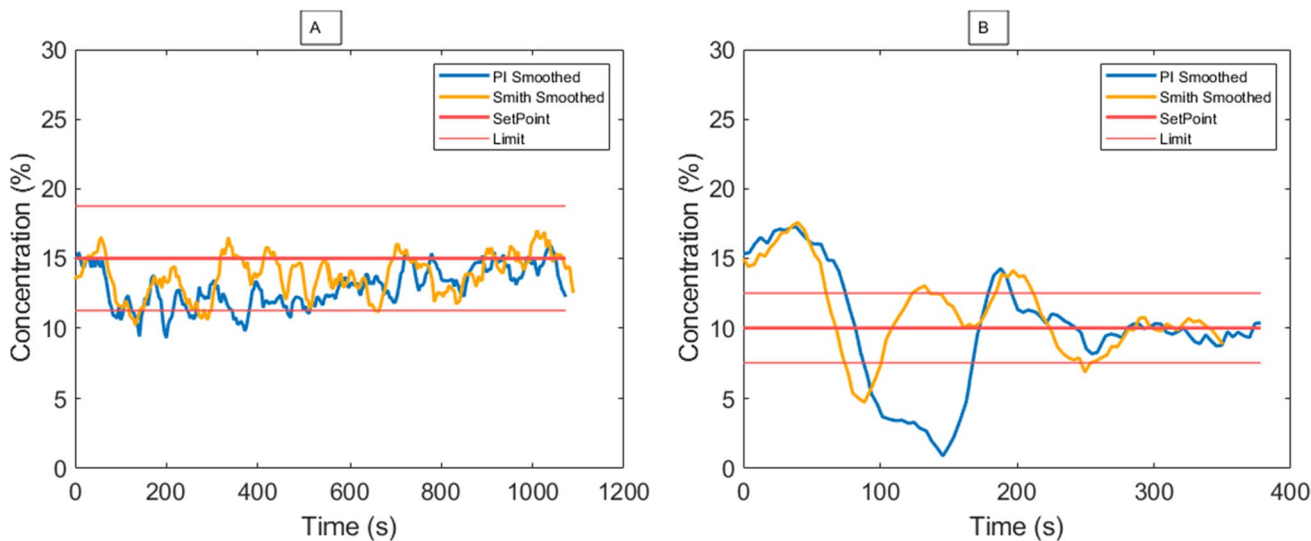


**Fig. 13** Comparison of the PI and the Smith predictor control structure on the ‘normal’ setup, with **A** the MCC step change and **B** the setpoint step change

## Conclusion

The RTD model of a dead time–dominated continuous powder blending system in the Smith predictor’s control structure has been successfully implemented. Compared to other control structures, which aim to reduce the effect of dead time, the presented control structure is straightforward and understandable. It contains the mechanistic RTD model of the system, broadening the use of this multipurpose tool, which proved to be essential in multiple steps of CM development. Aside from the model and the dead time, the controller has the same parameters as a simple PID controller. Tuning and testing of the controller are similar to the PID control.

The control structure was tested and compared to the PI control with step changes. The Smith predictor was generally faster, even at extreme conditions, while maintaining stable control of the concentration. Intensive tuning of the controllers was not part of this research, but both controllers could be further improved with fine-tuning. Another advantage of the Smith predictor is that it has a higher capacity to improve by tuning, as it has a wider stable space for control gains.

The use of active process controls, such as feedback controls in pharmaceutical lines, provides a high level of quality assurance and may be able to reduce waste significantly. The control structure is not limited to the powder blending process. The control of these processes is always challenging, but this is a generally applicable control method, with similar tuning to the well-established PID controls, providing a suitable solution to expanding the application of the RTD models.

**Funding** Open access funding provided by Budapest University of Technology and Economics. This work was supported by OTKA grant FK-143019. This work was supported by the ÚNKP-22–3-II-BME-171. New National Excellence Program of the Ministry for Innovation and Technology from the source of the National Research, Development and Innovation Fund. The research reported in this paper and carried out at BME has been supported by the National Laboratory of Artificial Intelligence funded by the NRDIO under the auspices of the Ministry for Innovation and Technology.

**Data Availability** The datasets generated during this work can be available upon request at the corresponding author.

## Declarations

**Conflict of Interest** The authors declare no competing interests.

**Open Access** This article is licensed under a Creative Commons Attribution 4.0 International License, which permits use, sharing, adaptation, distribution and reproduction in any medium or format, as long as you give appropriate credit to the original author(s) and the source, provide a link to the Creative Commons licence, and indicate if changes were made. The images or other third party material in this article are included in the article’s Creative Commons licence, unless indicated otherwise in a credit line to the material. If material is not included in the article’s Creative Commons licence and your intended use is not

permitted by statutory regulation or exceeds the permitted use, you will need to obtain permission directly from the copyright holder. To view a copy of this licence, visit <http://creativecommons.org/licenses/by/4.0/>.

## References

1. U.S. Food and Drug Administration. Guidance for industry, PAT-A framework for innovative pharmaceutical development, manufacturing and quality assurance [Internet]. FDA Off. Doc. 2004. Available from: <http://www.fda.gov/downloads/Drugs/GuidanceComplianceRegulatoryInformation/Guidances/ucm070305.pdf>.
2. Eifert T, Eisen K, Maiwald M, Herwig C. Current and future requirements to industrial analytical infrastructure—part 2: smart sensors. *Anal Bioanal Chem.* 2020;412:2037–45. Available from: <http://link.springer.com/10.1007/s00216-020-02421-1>.
3. Simon LL, Pataki H, Marosi G, Meemken F, Hungerbühler K, Baiker A, et al. Assessment of recent process analytical technology (PAT) trends: a multi-author review. *Org Process Res Dev.* 2015;19:3–62. Available from: <https://pubs.acs.org/doi/10.1021/op500261y>.
4. De Beer TRM, Bodson C, Dejaegher B, Walczak B, Vercauteren P, Burggraeve A, et al. Raman spectroscopy as a process analytical technology (PAT) tool for the in-line monitoring and understanding of a powder blending process. *J Pharm Biomed Anal.* 2008;48:772–9. Available from: <https://linkinghub.elsevier.com/retrieve/pii/S073170850800397X>.
5. De Beer T, Burggraeve A, Fonteyne M, Saerens L, Remon JP, Vervaeke C. Near infrared and Raman spectroscopy for the in-process monitoring of pharmaceutical production processes. *Int J Pharm.* 2011;417:32–47. <https://doi.org/10.1016/j.ijpharm.2010.12.012>.
6. Laske S, Paudel A, Scheibelhofer O, Sacher S, Hoermann T, Khinast J, et al. A review of PAT strategies in secondary solid oral dosage manufacturing of small molecules. *J Pharm Sci.* 2017;106:667–712. <https://doi.org/10.1016/j.xphs.2016.11.011>.
7. International Conference on Harmonization. ICH guideline Q8 (R2) on pharmaceutical development [Internet]. Regul. ICH. 2009. Available from: [http://www.ema.europa.eu/docs/en\\_GB/document\\_library/Scientific\\_guideline/2009/09/WC500002872.pdf](http://www.ema.europa.eu/docs/en_GB/document_library/Scientific_guideline/2009/09/WC500002872.pdf).
8. Roggo Y, Pauli V, Jelsch M, Pellegatti L, Elbaz F, Ensslin S, et al. Continuous manufacturing process monitoring of pharmaceutical solid dosage form: a case study. *J Pharm Biomed Anal.* 2020;179:112971. <https://doi.org/10.1016/j.jpba.2019.112971>.
9. Allison G, Cain YT, Cooney C, Garcia T, Bizjak TG, Holte O, et al. Regulatory and quality considerations for continuous manufacturing May 20–21, 2014 continuous manufacturing symposium. *J Pharm Sci.* 2015;104:803–12. <https://doi.org/10.1002/jps.24324>.
10. Lee SL, O’Connor TF, Yang X, Cruz CN, Chatterjee S, Madurawe RD, et al. Modernizing pharmaceutical manufacturing: from batch to continuous production. *J Pharm Innov.* 2015;10:191–9. Available from: <http://link.springer.com/10.1007/s12247-015-9215-8>.
11. Domokos A, Nagy B, Szilágyi B, Marosi G, Nagy ZK. Integrated continuous pharmaceutical technologies—a review. *Org Process Res Dev.* 2021;25:721–39. Available from: <https://pubs.acs.org/doi/10.1021/acs.oprd.0c00504>.
12. Démuth B, Fülöp G, Kovács M, Madarász L, Ficzer M, Kőte Á, et al. Continuous manufacturing of homogeneous ultralow-dose granules by twin-screw wet granulation. *Period Polytech Chem Eng.* 2020;64:391–400. Available from: <https://pp.bme.hu/ch/article/view/14972>.
13. Domokos A, Nagy B, Gyürkés M, Farkas A, Tacsik K, Pataki H, et al. End-to-end continuous manufacturing of conventional compressed tablets: from flow synthesis to tableting through integrated

- crystallization and filtration. *Int J Pharm.* 2020;581:119297. <https://doi.org/10.1016/j.ijpharm.2020.119297>.
14. Fisher AC, Liu W, Schick A, Ramanadham M, Chatterjee S, Brykman R, et al. An audit of pharmaceutical continuous manufacturing regulatory submissions and outcomes in the US. *Int J Pharm.* 2022;622:121778. <https://doi.org/10.1016/j.ijpharm.2022.121778>.
  15. International Conference on Harmonization. ICH Q13 continuous manufacturing of drug substances and drug products - Concept Paper. 2018.
  16. U.S. Food and Drug Administration. Quality considerations for continuous manufacturing guidance for industry draft guidance [Internet]. 2019. Available from: <https://www.fda.gov/Drugs/GuidanceComplianceRegulatoryInformation/Guidances/default.htm>.
  17. Gao Y, Muzzio FJ, Ierapetritou MG. A review of the residence time distribution (RTD) applications in solid unit operations. *Powder Technol.* 2012;228:416–23. <https://doi.org/10.1016/j.powtec.2012.05.060>.
  18. Bhalode P, Tian H, Gupta S, Razavi SM, Roman-Ospino A, Talebian S, et al. Using residence time distribution in pharmaceutical solid dose manufacturing – a critical review. *Int J Pharm.* 2021;610:121248. <https://doi.org/10.1016/j.ijpharm.2021.121248>.
  19. Beke ÁK, Gyürkés M, Nagy ZK, Marosi G, Farkas A. Digital twin of low dosage continuous powder blending – artificial neural networks and residence time distribution models. *Eur J Pharm Biopharm.* 2021;169:64–77. Available from: <https://linkinghub.elsevier.com/retrieve/pii/S0939641121002381>.
  20. Engisch W, Muzzio F. Using residence time distributions (RTDs) to address the traceability of raw materials in continuous pharmaceutical manufacturing. *J Pharm Innov.* 2016;11:64–81. Available from: <http://link.springer.com/10.1007/s12247-015-9238-1>.
  21. Gao Y, Vanarase A, Muzzio F, Ierapetritou M. Characterizing continuous powder mixing using residence time distribution. *Chem Eng Sci.* 2011;66:417–25. <https://doi.org/10.1016/j.ces.2010.10.045>.
  22. Gao Y, Muzzio FJ, Ierapetritou MG. Optimizing continuous powder mixing processes using periodic section modeling. *Chem Eng Sci.* 2012;80:70–80. <https://doi.org/10.1016/j.ces.2012.05.037>.
  23. Gyürkés M, Madarász L, Köte Á, Domokos A, Mészáros D, Beke ÁK, et al. Process design of continuous powder blending using residence time distribution and feeding models. *Pharmaceutics.* 2020;12:1119. Available from: <https://www.mdpi.com/1999-4923/12/11/1119>.
  24. Sebastian Escotet-Espinoza M, Moghtadernejad S, Oka S, Wang Y, Roman-Ospino A, Schäfer E, et al. Effect of tracer material properties on the residence time distribution (RTD) of continuous powder blending operations. Part I of II: Experimental evaluation. *Powder Technol.* 2019;342:744–63. <https://doi.org/10.1016/j.powtec.2018.10.040>.
  25. Muzzio F, Oka S. Using residence time distribution to understand continuous blending. *Powder Bulk Eng.* 2017.
  26. Oka S, Van Assche I, Futran M, Muzzio F, Escotet-Espinoza MS, Wang Z, et al. Effect of material properties on the residence time distribution (RTD) characterization of powder blending unit operations. Part II of II: Application of models. *Powder Technol.* 2018;344:525–44. <https://doi.org/10.1016/j.powtec.2018.12.051>.
  27. Kotamarthy L, Ramachandran R. Mechanistic understanding of the effects of process and design parameters on the mixing dynamics in continuous twin-screw granulation. *Powder Technol.* 2021;390:73–85. <https://doi.org/10.1016/j.powtec.2021.05.071>.
  28. Kumar A, Vercruyse J, Vanhoorne V, Toiviainen M, Panouillot PE, Juuti M, et al. Conceptual framework for model-based analysis of residence time distribution in twin-screw granulation. *Eur J Pharm Sci.* 2015;71:25–34. <https://doi.org/10.1016/j.ejps.2015.02.004>.
  29. Kumar A, Alakarjula M, Vanhoorne V, Toiviainen M, De Leersnyder F, Vercruyse J, et al. Linking granulation performance with residence time and granulation liquid distributions in twin-screw granulation: An experimental investigation. *Eur J Pharm Sci.* 2016;90:25–37. <https://doi.org/10.1016/j.ejps.2015.12.021>.
  30. Plath T, Korte C, Sivanapillai R, Weinhart T. Parametric study of residence time distributions and granulation kinetics as a basis for process modeling of twin-screw wet granulation. *Pharmaceutics.* 2021;13:645. Available from: <https://www.mdpi.com/1999-4923/13/5/645>.
  31. KashaniRahimi S, Paul S, Sun CC, Zhang F. The role of the screw profile on granular structure and mixing efficiency of a high-dose hydrophobic drug formulation during twin screw wet granulation. *Int J Pharm.* 2020;575:118958. <https://doi.org/10.1016/j.ijpharm.2019.118958>.
  32. Dülle M, Özcoban H, Leopold CS. Investigations on the residence time distribution of a three-chamber feed frame with special focus on its geometric and parametric setups. *Powder Technol.* 2018;331:276–85. <https://doi.org/10.1016/j.powtec.2018.03.019>.
  33. Furukawa R, Singh R, Ierapetritou M. Effect of material properties on the residence time distribution (RTD) of a tablet press feed frame. *Int J Pharm.* 2020;591:119961. <https://doi.org/10.1016/j.ijpharm.2020.119961>.
  34. Tanimura S, Singh R, Román-Ospino AD, Ierapetritou M. Residence time distribution modelling and in line monitoring of drug concentration in a tablet press feed frame containing dead zones. *Int J Pharm.* 2021;592:120048. Available from: <https://linkinghub.elsevier.com/retrieve/pii/S0378517320310334>.
  35. Tian G, Koolivand A, Gu Z, Orella M, Shaw R, O'Connor TF. Development of an RTD-based flowsheet modeling framework for the assessment of in-process control strategies. *AAPS PharmSciTech.* 2021;22:25. Available from: <http://link.springer.com/10.1208/s12249-020-01913-8>.
  36. Karttunen AP, Poms J, Sacher S, Sparén A, Ruiz Samblás C, Fransson M, et al. Robustness of a continuous direct compression line against disturbances in feeding. *Int J Pharm.* 2020;574:118882. <https://doi.org/10.1016/j.ijpharm.2019.118882>.
  37. Karttunen AP, Hörmann TR, De Leersnyder F, Ketolainen J, De Beer T, Hsiao WK, et al. Measurement of residence time distributions and material tracking on three continuous manufacturing lines. *Int J Pharm.* 2019;563:184–97. <https://doi.org/10.1016/j.ijpharm.2019.03.058>.
  38. Martínez MC, Karttunen AP, Sacher S, Wahl P, Ketolainen J, Khinast JG, et al. RTD-based material tracking in a fully-continuous dry granulation tableting line. *Int J Pharm.* 2018;547:469–79. <https://doi.org/10.1016/j.ijpharm.2018.06.011>.
  39. Gyürkés M, Madarász L, Záhonyi P, Köte Á, Nagy B, Pataki H, et al. Soft sensor for content prediction in an integrated continuous pharmaceutical formulation line based on the residence time distribution of unit operations. *Int J Pharm.* 2022;624:121950. Available from: <https://linkinghub.elsevier.com/retrieve/pii/S0378517322005051>.
  40. Bhaskar A, Singh R. Residence time distribution (RTD)-based control system for continuous pharmaceutical manufacturing process. *J Pharm Innov.* 2019;14:316–31. Available from: <http://link.springer.com/10.1007/s12247-018-9356-7>.
  41. Hörmann T, Horn M, Karttunen A-P, Rehr J, Nopens I, Korhonen O, et al. Control of three different continuous pharmaceutical manufacturing processes: use of soft sensors. *Int J Pharm.* 2018;543:60–72. <https://doi.org/10.1016/j.ijpharm.2018.03.027>.
  42. El-Hagrasy AS, Delgado-Lopez M, Drennen JK. A Process analytical technology approach to near-infrared process control of pharmaceutical powder blending: part II: qualitative near-infrared models for prediction of blend homogeneity. *J Pharm Sci.* 2006;95:407–21. Available from: <https://linkinghub.elsevier.com/retrieve/pii/S0022354916319499>.
  43. Kruijs J, Rehr J, Faulhammer E, Witschnigg A, Khinast JG. Material tracking in a continuous direct capsule-filling process

- via residence time distribution measurements. *Int J Pharm.* 2018;550:347–58. <https://doi.org/10.1016/j.ijpharm.2018.08.056>.
44. Krusz J, Rehl J, Sacher S, Aigner I, Horn M, Khinast JG. RTD modeling of a continuous dry granulation process for process control and materials diversion. *Int J Pharm.* 2017;528:334–44. <https://doi.org/10.1016/j.ijpharm.2017.06.001>.
  45. Vargas JM, Nielsen S, Cárdenas V, Gonzalez A, Aymat EY, Almodovar E, et al. Process analytical technology in continuous manufacturing of a commercial pharmaceutical product. *Int J Pharm.* 2018;538:167–78. <https://doi.org/10.1016/j.ijpharm.2018.01.003>.
  46. Destro F, Barolo M. A review on the modernization of pharmaceutical development and manufacturing – trends, perspectives, and the role of mathematical modeling. *Int J Pharm.* 2022;620:121715. <https://doi.org/10.1016/j.ijpharm.2022.121715>.
  47. Hopkins M. LOSS in weight feeder systems. *Meas Control.* 2006;39:237–40.
  48. Bostijn N, Dhondt J, Ryckaert A, Szabó E, Dhondt W, Van Snick B, et al. A multivariate approach to predict the volumetric and gravimetric feeding behavior of a low feed rate feeder based on raw material properties. *Int J Pharm.* 2019;557:342–53. <https://doi.org/10.1016/j.ijpharm.2018.12.066>.
  49. Hanson J. Control of a system of loss-in-weight feeders for drug product continuous manufacturing. *Powder Technol.* 2018;331:236–43. <https://doi.org/10.1016/j.powtec.2018.03.027>.
  50. Destro F, García Muñoz S, Bezzo F, Barolo M. Powder composition monitoring in continuous pharmaceutical solid-dosage form manufacturing using state estimation – proof of concept. *Int J Pharm.* 2021;605:120808. Available from: <https://linkinghub.elsevier.com/retrieve/pii/S037851732100613X>.
  51. Nagy B, Farkas A, Gyürkés M, Komaromy-Hiller S, Démuth B, Szabó B, et al. In-line Raman spectroscopic monitoring and feedback control of a continuous twin-screw pharmaceutical powder blending and tableting process. *Int J Pharm.* 2017;530:21–9. Available from: <https://linkinghub.elsevier.com/retrieve/pii/S0378517317306403>.
  52. Reimers T, Thies J, Stöckel P, Dietrich S, Pein-Hackelbusch M, Quodbach J. Implementation of real-time and in-line feedback control for a fluid bed granulation process. *Int J Pharm.* 2019;567:118452. <https://doi.org/10.1016/j.ijpharm.2019.118452>.
  53. Jelsch M, Roggo Y, Kleinebudde P, Krumme M. Model predictive control in pharmaceutical continuous manufacturing: a review from a user's perspective. *Eur J Pharm Biopharm.* 2021;159:137–42. <https://doi.org/10.1016/j.ejpb.2021.01.003>.
  54. Singh R, Ierapetritou M, Ramachandran R. System-wide hybrid MPC – PID control of a continuous pharmaceutical tablet manufacturing process via direct compaction. *Eur J Pharm Biopharm.* 2013;85:1164–82. <https://doi.org/10.1016/j.ejpb.2013.02.019>.
  55. Sen M, Singh R, Ramachandran R. A hybrid MPC-PID control system design for the continuous purification and processing of active pharmaceutical ingredients. *Processes.* 2014;2:392–418. Available from: <http://www.mdpi.com/2227-9717/2/2/392>.
  56. Mesbah A, Paulson JA, Lakerveld R, Braatz RD. Model predictive control of an integrated continuous pharmaceutical manufacturing pilot plant. *Org Process Res Dev.* 2017;21:844–54. Available from: <https://pubs.acs.org/doi/10.1021/acs.oprd.7b00058>.
  57. Biegler LT, Yang X, Fischer GAG. Advances in sensitivity-based nonlinear model predictive control and dynamic real-time optimization. *J Process Control.* 2015;30:104–16. <https://doi.org/10.1016/j.jprocont.2015.02.001>.
  58. Rehl J, Krusz J, Sacher S, Khinast J, Horn M. Optimized continuous pharmaceutical manufacturing via model-predictive control. *Int J Pharm.* 2016;510:100–15. <https://doi.org/10.1016/j.ijpharm.2016.06.024>.
  59. Normey-Rico JE, Camacho EF. Dead-time compensators: a survey. *Control Eng Pract.* 2008;16:407–28. Available from: <https://linkinghub.elsevier.com/retrieve/pii/S0967066107001141>.
  60. Hang CC, Wang QG, Yang XP. A modified Smith predictor for a process with an integrator and long dead time. *Ind Eng Chem Res.* 2003;42:484–9.
  61. Santacesaria C, Scattolini R. Easy tuning of smith predictor in presence of delay uncertainty. *Automatica.* 1993;29:1595–7.
  62. Astrom KJ, Hang CC, Lim BC. A new Smith predictor for controlling a process with an integrator and long dead-time. *IEEE Trans Automat Contr.* 1994;39:343–5. Available from: <http://ieeexplore.ieee.org/document/272329/>.
  63. McMillan GK. Performance comparison between a Smith predictor and a Pid controller for control valve hysteresis and process non-self-regulation. *Proc Am Control Conf.* 1983;1:343–8.
  64. SigurdSkogestad CG. Should we forget the Smith predictor? *IFAC-PapersOnLine.* 2018;51:769–74. <https://doi.org/10.1016/j.ifacol.2018.06.203>.
  65. Mizsey P. *Folyamatirányítási rendszerek.* 1st ed. Budapest: Typotex; 2011.

**Publisher's Note** Springer Nature remains neutral with regard to jurisdictional claims in published maps and institutional affiliations.